Chalcogenide Letters Vol. 16, No. 5, May 2019, p. 231 - 239

SYNTHESIS AND CHARACTERIZATION OF CHEMICALLY SPRAYED Cu_2CoSnS_4 THIN FILMS

M. A. AHMED, N. A. BAKR, A. A. KAMIL
Department of Physics, College of Science, University of Diyala, Diyala, Iraq

Cu_2CoSnS_4 (CCTS) films were deposited by using chemical spray pyrolysis technique at substrate temperature (400 ±10)℃ and thickness of about (350 ±10) nm using copper chloride dihydrate ($CuCl_2.2H_2O$), cobalt chloride hexahydrate ($CoCl_2.6H_2O$), tin chloride pentahydrate ($SnCl_4.5H_2O$) and thiourea ($SC(NH_2)_2$ as sources of copper, cobalt, tin, and sulfur ions respectively. The influence of thiourea concentration on the structural, morphological, optical and electrical properties of these films have been investigated using GIXRD, Raman spectroscopy, FESEM, UV-Visible spectrophotometry and Hall Effect measurements. The XRD results showed that all films are polycrystalline in nature with tetragonal stannite structure and preferred orientation along (204) plane. The crystallite size (D) of all samples was calculated using Scherrer's equation and it is found that the sample deposited at thiourea concentration of 0.16 M has maximum crystallite of 12.88 nm, while it was minimum (5.09) nm for the sample prepared at thiourea concentration of (0.22) M. Raman spectroscopy analysis confirms the purity of the films formation phase. The main peak of Raman Shift of all samples is located at (321-325) cm^{-1} attributed to the stannite CCTS structure. This peak arises from A1 vibration mode, where only S-anions. The FESEM results showed the appearance of nanoparticles with different shapes and sizes. The optical energy band gap (E_g) for allowed direct electronic transition was calculated using Tauc's plot. It is found that the energy band gap (E_g) is in the range of (1.3-1.85) eV. The Hall Effect measurement shows that all films are P-type and the highest conductivity value was (0.4174 $\Omega.cm^{-1}$) for CCTS4 film corresponding to the highest mobility in the value of (1.822 $cm^2/V.s$). These results suggest that the deposited films are good candidate for absorber layer in solar cells.

(Received March 2, 2019; Accepted May 21, 2019)

Keywords: Cu_2CoSnS_4 thin films, Chemical spray pyrolysis, Structural properties, FESEM, Optical properties, Hall effect

1. Introduction

In order to meet the growing demand for, clean and renewable energy from solar cells, the researchers' efforts have been directed towards preparing new materials that enable the production of solar energy to generate electricity [1]. Attempting to replace crystallized silicon due to less expensive semiconductor materials through the preparation of absorbent layers (effective layer) using thin film technology [2]. Yet more than 80% of the world's energy is produced by fossil fuels (coal, oil, and natural gas), where excessive use of this fuel has polluted the environment [3]. Quaternary chalcogenide semiconductor based on earth abundant elements have become the subject of intensive research interest for researchers because they are made up of available and nontoxic elements and have an ideal energy gap for many optical applications. Most of the researchers studied Cu_2CoSnS_4, one of the compounds of the semiconductor family Cu-II2- III-VI4, [4]. The CCTS films are still challenging because CCTS is a very complex compound, and it is often difficult to control the process of growth during preparation. However, the CCTS films have recently been successfully used in photovoltaic applications using different deposition techniques such as solvothermal [5], sol-gel [1,6], Hot-injection [7], electrospinning [8], high temperature route and thermal chemical decomposition method [9]. Given the importance of CCTS in many applications and in many areas, we have considered the effect of sulfur concentration in the CCTS films by chemical spray pyrolysis method.

*Corresponding author: nabeelalibakr@yahoo.com

2. Experimental

Cu_2CoSnS_4 (CCTS) thin films were deposited on glass substrates by chemical spray pyrolysis. The glass substrates were ultrasonically cleaned in distilled water, acetone, and distilled water respectively for (10 min) of each step and then dried by blowing them with filtered air. Sprayed solution was prepared by mixing aqueous solutions of copper chloride dihydrate ($CuCl_2.2H_2O$), cobalt chloride hexahydrate ($CoCl_2.6H_2O$) and tin chloride dihydrate ($SnCl_2.2H_2O$) with concentrations of 0.04 M, 0.02 M and 0.02 M respectively. The thiourea ($SC(NH_2)_2$) concentration was varied according to the values shown in Table (1). Excess thiourea was used to substitute the loss of sulphur during the heating process. The solutions were well mixed by magnetic stirrer and the final solution was left for one hour to make sure that no residues are left. The deposition process was carried out using a homemade system at a substrate temperature of 400 ˚C using filtered air as carrier gas at a flow rate approximately to 5 mL/min. Other deposition parameters are described elsewhere [10]. The resultant films have good adhesive properties with a uniform thickness of (350) nm measured by gravimetric method and confirmed by cross section image of the films using FESEM as shown in Figure (1). The structural properties were investigated by using Grazing Incidence X-Ray Diffraction (GIXRD) (Ultima IV X-Ray diffractometer) with CuKα radiation (λ = 1.5406 Å) as the source. Topography of the surface of the deposited films was imaged using FESEM (MIRA3, TE-SCAN). Raman Spectra were recorded at backscattering configuration using (Jobin-Yvon Horiba Labram800). The optical transmission and absorption spectra of the films were recorded by (Shimadzu, UV- 1800) in the wavelength range of (350 – 900) nm. Hall Effect measurements were conducted by using (HMS 3000).

Table 1. Molar concentrations of thiourea used to prepare CCTS films.

Sample Code	$SC(NH_2)_2$ M
CCTS1	0.10
CCTS2	0.12
CCTS3	0.14
CCTS4	0.16
CCTS5	0.18
CCTS6	0.20
CCTS7	0.22

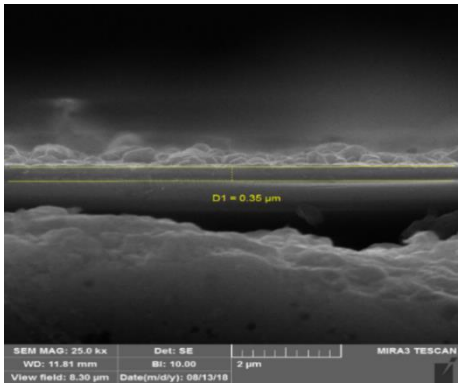

Fig. 1. Cross section image of typical CCTS film.

3. Results and discussion

XRD results showed that all deposited thin films have tetragonal (Stannite) structure with preferred orientation of (204). Figure (2) shows the diffraction patterns with clear peaks at (2θ~ 28.5°, 33.1°, 47.5°, 56.4° and 69.4°) which correspond to (112), (004), (204) (312) and (400) respectively. The results well match the standard card (ICDD No. 26-0513) with the absence of the peaks of the compounds such as Cu_2S, SnS, Cu_3SnS_4 and other phases. Table (2) shows the XRD results of the CCTS thin films.

According to conventional Scherrer's formula [11]:

$$D = \frac{K\lambda}{\beta \cos\theta} \tag{1}$$

The crystallite size in the favorite direction (204) reached the maximum value (12.88 nm) for the sample CCTS4. There is a significant difference in crystallite size, which may be due to the different chemical homogeneity of the material, which greatly affects the size of the crystals and possibly the nucleation rate of the CCTS molecules [12]. The texture coefficient (Tc) represents the texture of a particular plane, in which greater than unity values imply that there are numerous of grains in that particular direction. The texture coefficients Tc(*hkl*) for all samples have been calculated from the X-ray data using the well-known formula [13]:

$$T_c(hkl) = \frac{I(hkl)/I_o(hkl)}{N_r^{-1}\sum I(hkl)/I_o(hkl)} \tag{2}$$

where I(hk*l*) is the measured intensity, I_o(hk*l*) taken from the (ICDD), (N_r) is the number of reflections and (hk*l*) is Miller indices. The texture coefficient is calculated for crystal plane (204) of the CCTS thin films. The texture coefficient T_c values are (>1) for all films indicating that there are numerous grains in the (204) favorite direction. The estimated lattice parameters (a and c) values are in agreement with theoretical values (a = 5.402 Å and c = 10.80 Å). In ideal tetragonal structure, the ratio of the lattice vector (c/a) is 2. In the present work three cases are noticed. First, the ratio is greater than 2 (as for the samples CCTS1, CCTS2 and CCTS3), indicating that the lattice is elongated along the c-axis, second, the ratio is less than 2 (as for the samples CCTS5, CCTS6 and CCTS7), which implies that the lattice is compressed in the c-axis direction, and the third case for the sample CCTS4 which indicates ideal tetragonal structure. Table (2) also shows the unit cell volume of all samples and it can be seen that the sample CCTS4 has the nearest value (315.22 $Å^3$) to the theoretical one (315.31 $Å^3$).

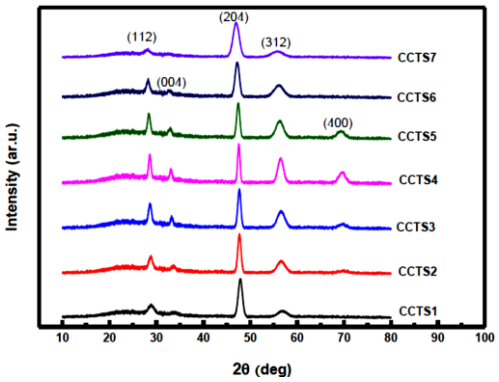

Fig. 2. X-ray diffraction patterns of CCTS thin films

Table 2. X-ray diffraction results of the CCTS thin films.

Sample	2θ (deg)	D (nm)	$T_{c\,(204)}$	Lattice Constants (Å)		c/a	Unit Cell Volume ($Å^3$)
				a=b	c		
CCTS1	47.8	5.49	1.77	5.27	10.94	2.07	303.84
CCTS2	47.6	7.57	1.19	5.30	10.95	2.06	307.59
CCTS3	47.6	10.42	1.26	5.43	10.96	2.01	323.15
CCTS4	47.5	12.88	1.03	5.40	10.81	2.00	315.22
CCTS5	47.5	11.31	1.25	5.39	10.84	2.01	314.92
CCTS6	47.3	7.03	1.55	5.53	10.66	1.92	325.99
CCTS7	47.0	5.09	2.00	5.48	10.84	1.97	325.53

To investigate the phase purity of Cu_2CoSnS_4 films, Raman shift measurements were carried out and the results are plotted in figure (3). It can be observed that the spectra of all samples are not symmetric suggesting that each spectrum is composed of more than one peak which can be analyzed by deconvolution process. The results of this process are depicted in table (3) which shows that the main peak of the samples is located at (321-325) cm^{-1} attributed to the stannite CCTS structure. These peaks arise from A1 vibration mode, where only S-anions are involved [17]. The lower intense peak near 287 cm^{-1} is also assigned to Cu_2CoSnS_4 compound [14,15]. The samples CCTS3 and CCTS6 showed peaks at (305) cm^{-1} and (300) cm^{-1} respectively. Previous reports assigned these peaks to the formation of CCTS single phase [16,12]. These results are in agreement with the results obtained by XRD where no secondary phases had been observed.

Table 3. Results of Raman analysis.

Sample	Peak Center (cm^{-1})	Peak Width (cm^{-1})	Intensity (ar. u.)
CCTS1	321	30.85	62.733
	286	36.42	18.874
CCTS2	322	26.39	71.530
	287	34.02	17.480
CCTS3	325	23.88	61.078
	305	47.81	21.118
CCTS4	324	24.31	81.057
	287	28.04	14.814
CCTS5	324	25.59	77.836
	287	24.58	15.606
CCTS6	324	25.30	61.762
	300	49.40	22.271
CCTS7	322	28.67	66.680
	287	35.64	18.252

Topography of the surface of the materials deposited as thin films is studied using FESEM, which enables the imaging of the surface of the materials with high magnification and precision. Figs. 4 a and b show the SEM micrographs magnified by 150 kx for CCTS thin films prepared with the different concentrations of thiourea at (400 ˚C) substrate temperature. Different shapes and structures can be seen where Cauliflower-like with irregular particle size is dominated. There are also some areas containing polyhedral shapes with secondary growth and voids [4], which means that a new layer starts to grow before the completion of the growth of the layer beneath it. The grain boundaries are also visible. The average grain size is calculated by average grain intercept (AGI) method using ImageJ software and the results are depicted in Table 4.

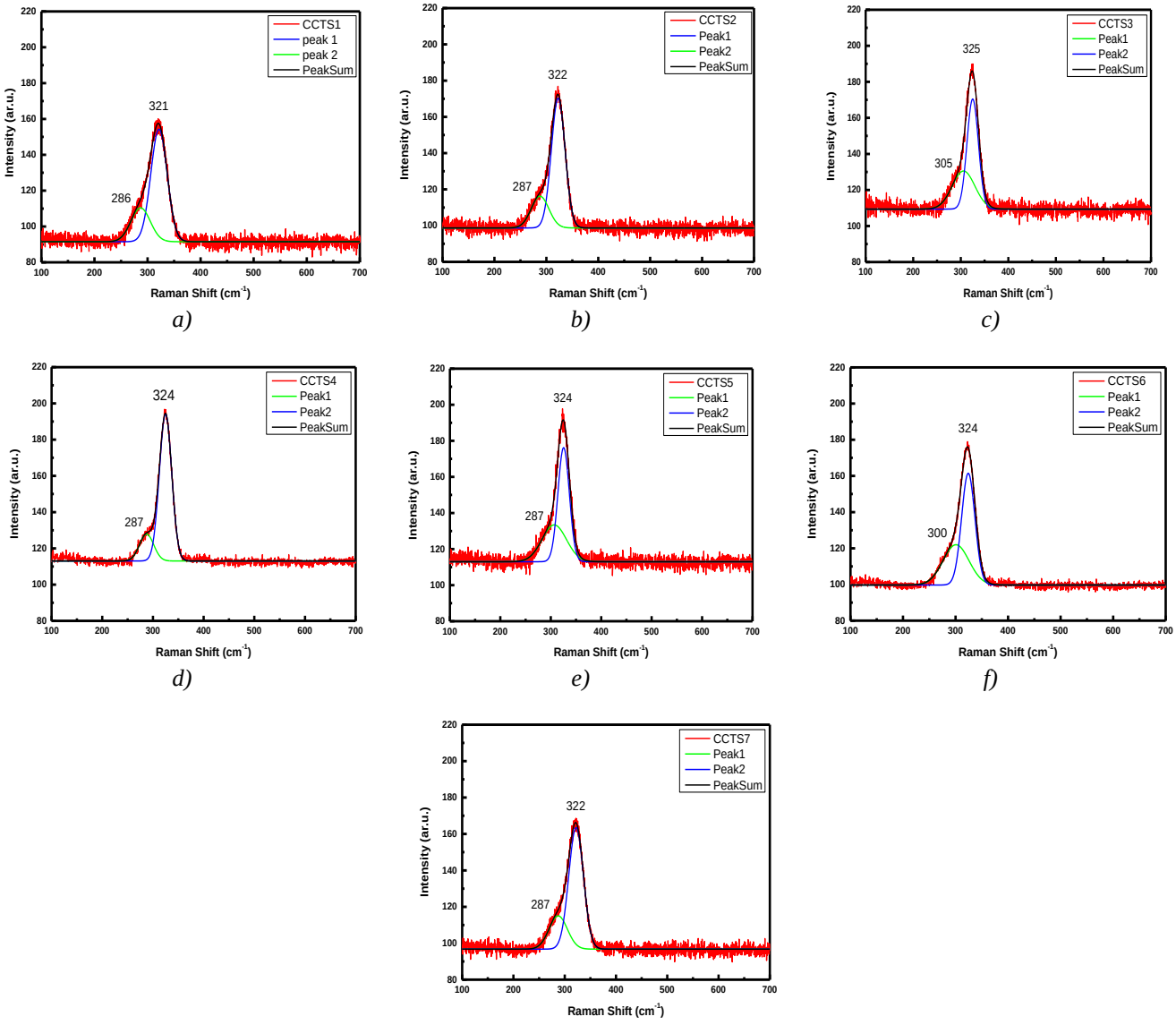

Fig. 3 Raman spectrum for thin film of a)CCTS1; b) CCTS2; c) CCTS3; d) CCTS4; e) CCTS5; f) CCTS6; and g) CCTS7

Sample	CCTS1	CCTS2	CCTS3	CCTS4	CCTS5	CCTS6	CCTS7
Average Particle Size (nm)	24.86	21.78	19.53	22.71	18.30	20.02	14.05

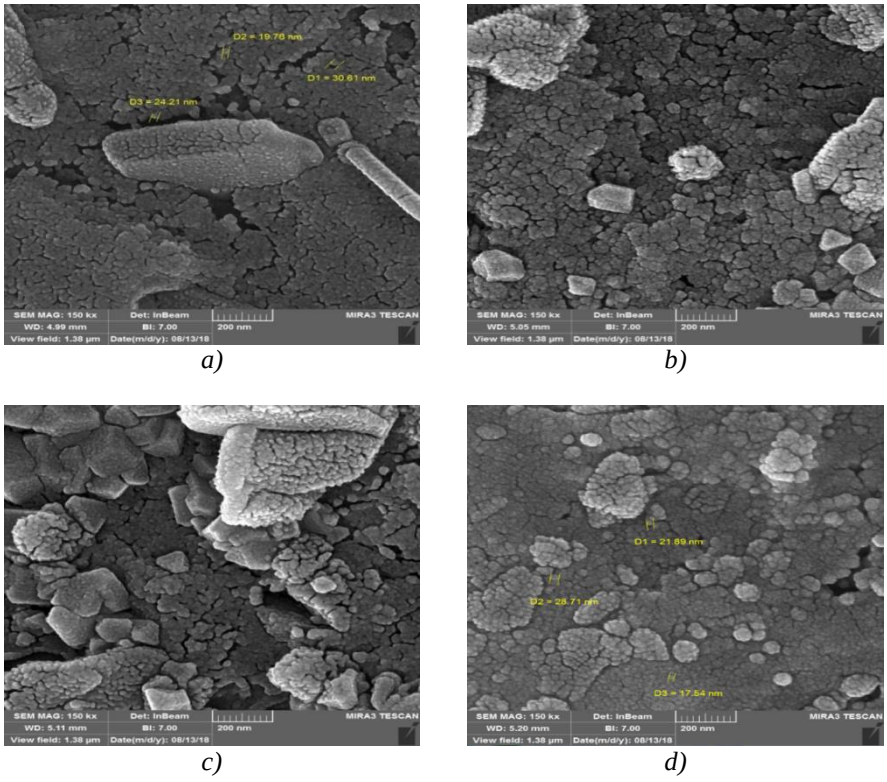

Fig. 4 a. FESEM images of a) CCTS1, b) CCTS2, c) CCTS3 and d) CCTS4.

Optical absorption spectra of the films in the spectral range of (300 – 900) nm were recorded by using UV–visible spectrophotometer. The analysis of the dependence of absorption coefficient on photon energy in the high absorption regions is performed to obtain the detailed information about the energy band gaps of the films where the optical energy band gap (E_g) can be estimated by the well-known formula:

$$\alpha h\nu = A\,(h\nu - E_g)^r \tag{3}$$

where α is the absorption coefficient, hν is the photon energy, E_g is the optical band gap, A is a constant which does not depend on photon energy and r has four numeric values (1/2) for allowed direct, 2 for allowed indirect, 3 for forbidden direct and (3/2) for forbidden indirect optical transitions. In this work, direct band gap was determined plotting a graph between $(\alpha h\nu)^2$ and (hν) in eV, where a straight line is obtained. The extrapolation of this straight line to $(\alpha h\nu)^2 = 0$ gives value of the direct band gap of the material, and this is shown in figure (5). The energy gap obtained for CCTS samples is in the range of (1.3-1.85) eV as shown in table (5) which is in agreement with other studies [16]. The energy gap is one of the important factors to improve the efficiency of solar cells made of CCTS as an active layer and the obtained values make these films good candidates in solar cells applications.

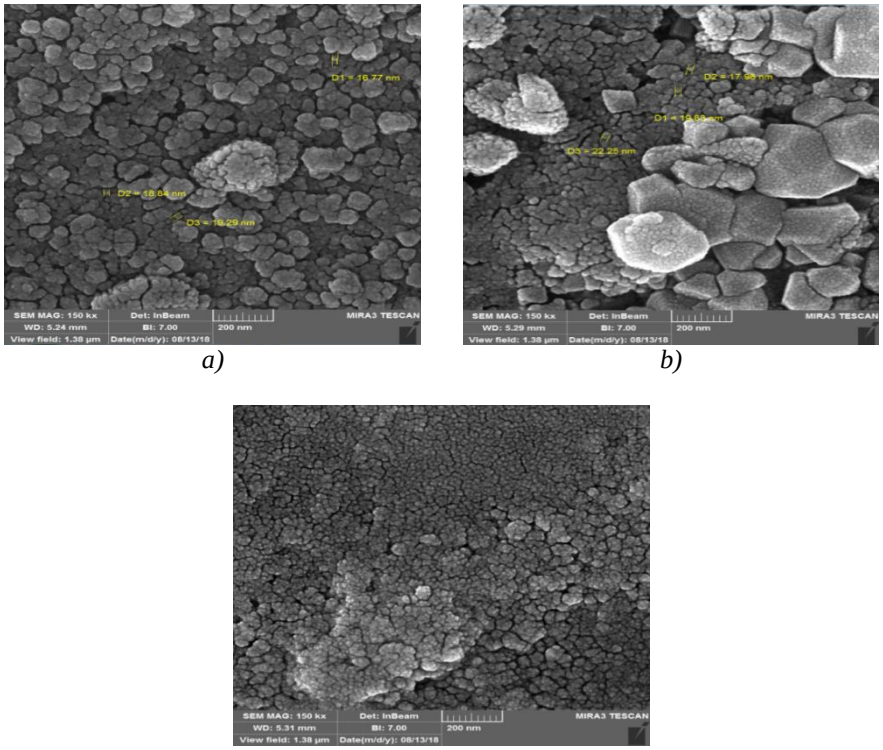

a) *b)*

c)

Fig. 4 b. FESEM images of CCTS5, CCTS6 and CCTS7.

Table 5. Values of optical energy band gap of CCTS.

Sample	E_g (eV)
CCTS1	1.39
CCTS2	1.38
CCTS3	1.30
CCTS4	1.53
CCTS5	1.65
CCTS6	1.74
CCTS7	1.85

Hall Effect measurement at room temperature for CCTS thin films was carried oput, and it was used to determine the type, concentration, mobility of the majority carriers and the conductivity. The measured values are depicted in table (6). The highest value of electrical conductivity is (0.4174 $\Omega.cm^{-1}$) of the CCTS4 thin film. From Hall coefficient sign it is confirmed that all CCTS thin films are of P-type.

Table 6. Results of Hall Effect measurement.

Sample	R_H (cm^3/C)	n (cm^{-3})	μ (cm^2/V.s)	ρ (Ω.cm)	σ ($\Omega.cm^{-1}$)
CCTS1	11.3276	5.51×10^{17}	0.414	27.3614	0.0365
CCTS2	7.9917	7.81×10^{17}	1.121	7.1291	0.1402
CCTS3	5.1583	1.21×10^{18}	1.526	3.3803	0.2958
CCTS4	4.3648	1.43×10^{18}	1.822	2.3956	0.4174
CCTS5	7.6023	8.21×10^{17}	1.611	4.719	0.2119
CCTS6	9.9705	6.26×10^{17}	1.212	8.2265	0.1215
CCTS7	10.368	6.02×10^{17}	0.668	15.5209	0.0644

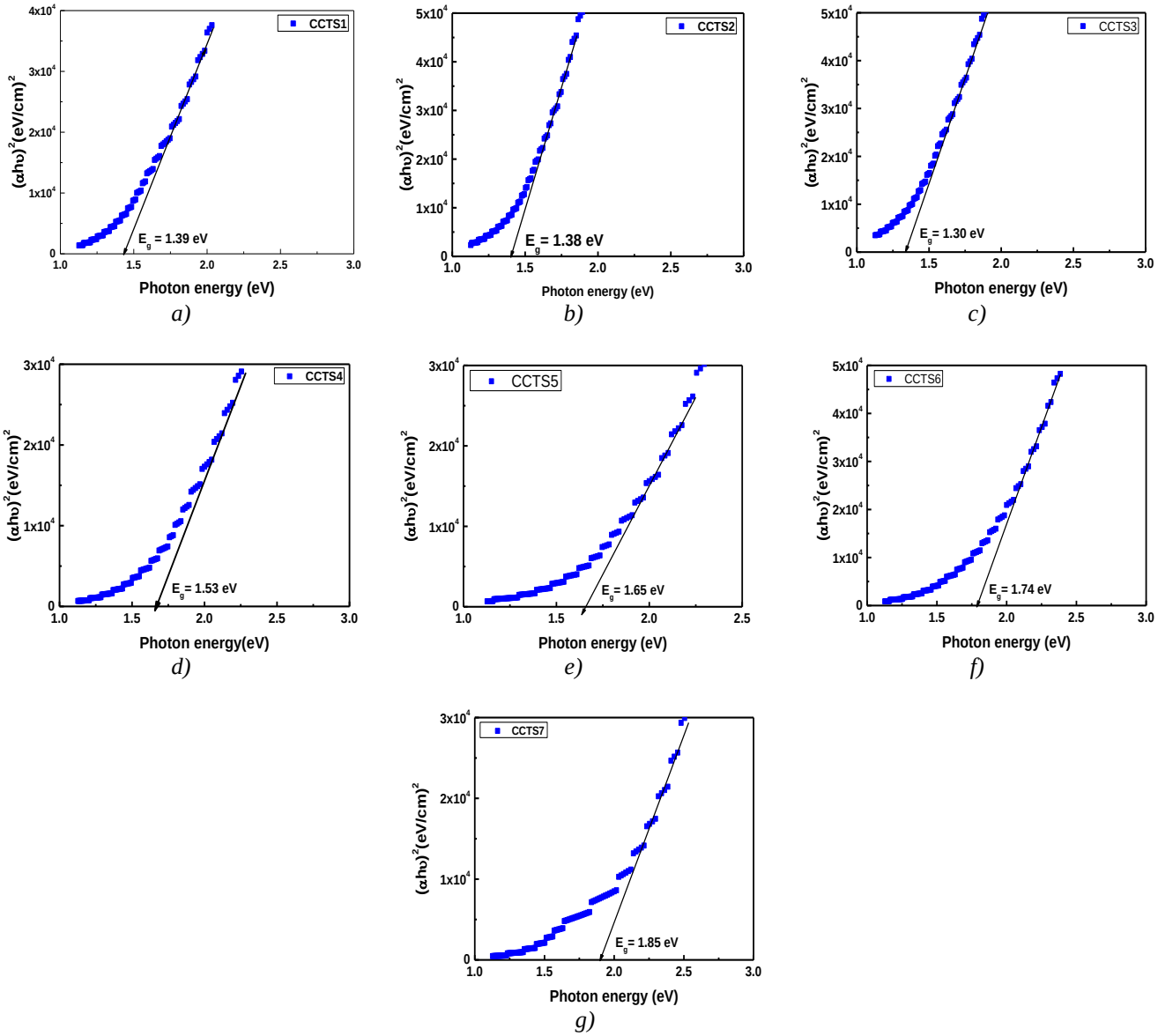

Fig. 5 g. The relation between $(ahv)^2$ and (hv) for thin film o a)CCTS1; b) CCTS2; c) CCTS3; d) CCTS4; e) CCTS5; f) CCTS6; and g) CCTS7

4. Conclusions

Thin films of Cu_2CoSnS_4 were deposited by spray pyrolysis method on clean preheated glass substrates at 400 °C with different concentrations of thiourea. The XRD results showed that all films are polycrystalline in nature with tetragonal structure and preferred orientation along (204) plane. The Raman spectra showed a major peak of CCTS at (321-325 cm^{-1}) which proves the formation stannite phase of CCTS. The prepared films have energy band gap very close to the optimum value of the band gap required for the absorber material in thin film solar cell. The conductivity of the films is estimated by Hall measurement and its maximum value is 0.4174 $(\Omega.cm)^{-1}$ for the film CCTS4 which can be considered to be suitable for solar cell applications.

References

[1] B. Murali, M. Madhuri, S.B. Krupanidhi, Journal of Applied physics **114**(14), 144312 (2013).
[2] J. L. Shay, J. H. Wernick, Ternary chalcopyrite semiconductors: growth, electronic properties, and applications: international series of monographs in the science of the solid state, Elsevier, 2017 Jul 26.
[3] M. Krishnaiah, P. Bhargava, S. Mallick, RSC Advances **5**(117), 96928 (2015).
[4] P. S. Maldar, M. A. Gaikwad, A. A. Mane, S. S. Nikam, S. P. Desai, S. D. Giri, A. Sarkar, A. V. Moholkar, Solar Energy **1**(158) 89 (2017)
[5] L. Shi, Y. Li, H. Zhu, Q. Li, Chem. Plus Chem. **79**(11), 1638 (2014).
[6] A. Sharma A, R. Thangavel, Cost-effective fabrication of Cu_2CoSnS_4 thin films for photovoltaic applications, In 2018 3rd International Conference on Microwave and Photonics (ICMAP) (pp. 1-2). IEEE, (2018 Feb 9).
[7] A. Gupta, K. Mokurala, A. Kamble, S. Shankar, S. Mallick, P. Bhargava, InAIP Conference Proceedings **1665**(1), 140022 (2015).
[8] F. Ozel, Journal of Alloys and Compounds **5**(657), 157 (2016).
[9] Y. Cui, R. Deng, G. Wang, D. Pan, Journal of Materials Chemistry **22**(43), 23136 (2012).
[10] N. A. Bakr, S. A. Salman, S. A. Hameed, International Journal of Applied Engineering Research **13**(6), 3379 (2018)
[11] N. A. Bakr, Z. T. Khodair, H. I. Mahdi, International Journal of Materials Science and Application **5**(6), 261 (2016).
[12] M. Benchikri, O. Zaberca, R. El Ouatib, B. Durand, F. Oftinger, A. Balocchi, J. Y. Chane-Ching, Materials Letters **1**(68), 340 (2012).
[13] N. A. Bakr, Z. T. Khodair, S. M. Hassan, Effect of substrate temperature on structural and optical properties of Cu2ZnSnS4 (CZTS) films prepared by chemical spray pyrolysis method, Research Journal of Chemical Sciences ISSN 2231:606X, (2015)
[14] P. R. Ghediya, T. K. Chaudhuri, Materials Research Express **5**(8), 085509 (2018).
[15] T. Wang, Q. Zhan, W. Cheng, Journal of Materials Science: Materials in Electronics 1-7.
[16] A. Ghosh, A. Biswas, R. Thangavel, G. Udayabhanu, RSC Advances **6**(98), 96025 (2016).
[17] A. H. Pinto, Green chemistry Approach for the synthesis of transition metal sulfide based on Cu_2ZnSnS_4(CZTS) and etching of their Impurities, Ph.D. Thesis, University of Minnesota, (2017).